(1961).
[14]I. Korobkin and Z. I. Slawsky, J. Chem. Phys. 37, 226 (1962).
[15]N. P. Carleton and T. R. Lawrence, Phys. Rev. 109, 1159 (1958).
[16]S. H. Neff and N. P. Carleton, Atomic Collision Processes, edited by M. R. C. McDowell (North-Holland Publishing Co., Amsterdam, 1964), p. 652.
[17]K. C. Clark and A. E. Belon, J. Atmospheric Terrest. Phys. 16, 205 (1959).
[18]A. L. Schmeltekopf, F. C. Fehsenfeld, G. I. Gilman, and E. E. Ferguson, Planetary Space Sci. 15, 401 (1967).
[19]A. L. Schmeltekopf, E. E. Ferguson, and F. C. Fehsenfeld, J. Chem. Phys. 48, 2966 (1968).

PHYSICAL REVIEW VOLUME 177, NUMBER 1 5 JANUARY 1969

Ejected Electron Distributions*

J. D. Garcia
Physics Department, University of Arizona, Tucson, Arizona 85721
(Received 29 July 1968)

Differential cross sections for production of secondary electrons in the ionization of atoms by charged-particle impact are examined in the classical binary-encounter approximation. General scalable expressions are given for both electron and heavy-charged-particle impact, and are compared with experimental and quantum treatments where possible. It is found that this formulation provides simple physical explanations of most features of ejected electron energy and velocity distributions. Proton-impact results are found to be in excellent agreement with experiment, and the electron-impact results converge to the Born results as expected.

I. INTRODUCTION

Previous work[1-5] has established that the classical binary-encounter approximation provides reasonable estimates of the total ionization cross sections of atoms and simple diatomic molecules, for almost all incident energies. This is not surprising, since the ionization process is one in which the correspondence principle can be applied.[6] Interest in the classical results is due in part to the ease of formulation, especially for systems such that even the Born approximation becomes intractable. Such a model, however, also enables us to extract more simply the physical explanations for the major features of the results,[2] if the model is quantitatively reliable.

The differential cross sections for secondary electron production provide a more sensitive test of the reliability and limitations of the classical binary-encounter approximation than do total cross sections. It is possible, for example, that the classical formulation approximates the total phase space reasonably, but does so by having fortuitous cancellations, so that the differentials would be incorrect. It is found, however, that at least the energy and speed distributions of the ejected electrons can be reasonably well predicted on this model.

In Sec. II, we present the formulation of the differential cross sections and discuss appropriate averages over bound electron properties. General, scalable expressions are obtained for both heavy particle and electron impact. Section III contains a comparison with existing experimental results. The discussion in Sec. IV includes some remarks on the application to general atomic systems. The proton results are found to be in good agreement with experiment. No experimental results are available for electron impact, but a comparison with Born results indicates the expected convergence for excited-state ionization.

II. ENERGY AND SPEED PROFILES

The binary-encounter approximation is based on the assumption that the dominant interaction is that between the incident charged particle and the atomic electrons.[1] It requires a knowledge of the differential cross section for the exchange of energy ΔE in the laboratory frame between the incident particle of mass m_1, charge Ze, and velocity $\vec{v}_1$, and the bound electron whose initial velocity is $\vec{v}_2$. The correct classical expression for this cross section, when averaged over all orientations of $\vec{v}_2$, for $m_1 \geq m_e$, is[7]

$$\frac{d\sigma^{\text{eff}}}{d\Delta E} = \frac{\pi}{3}\frac{(Ze^2)^2}{(\Delta E)^3}\frac{3v_2'^2+v_2^2}{v_1^2}, \quad 0<\Delta E<b;$$

$$= \frac{\pi}{6}\frac{(Ze^2)^2}{(\Delta E)^3}\frac{(v_1+v_1')^3+(v_2-v_2')^3}{v_1^2 v_2},$$

$$b<\Delta E<a;$$

$$= \frac{\pi}{3}\frac{(Ze^2)^2}{(\Delta E)^3}\frac{v_1'(v_1'^2+3v_1^2)}{v_1^2 v_2}, \quad \Delta E > a,$$

$$2m_e v_2 > (m_1 - m_e)v_1;$$

$$= 0, \quad \Delta E > a, \quad 2m_e v_2 < (m_1 - m_e)v_1; \tag{1}$$

where

$$a = \frac{4m_1 m_e}{(m_1+m_e)^2}[E_1 - E_2 + \tfrac{1}{2}v_1 v_2(m_1 - m_e)],$$

$$b = \frac{4m_1 m_e}{(m_1+m_e)^2}[E_1 - E_2 - \tfrac{1}{2}v_1 v_2(m_1 - m_e)],$$

$$v_1' = \left(v_1^2 - \frac{2\Delta E}{m_1}\right)^{1/2}, \quad v_2' = \left(v_2^2 + \frac{2\Delta E}{m_e}\right)^{1/2}.$$

Here E_1 is the projectile energy and E_2 the target-electron kinetic energy.

To be explicitly clear in what follows, we recall that the total cross sections for ionization are obtained from (1) as follows:

$$\sigma_{\text{ion}} = \sum_i n_i \int_{u_i}^{E_1} \frac{d\sigma(v_1 v_{2i})}{d\Delta E}\, d\Delta E, \tag{2}$$

where n_i is the number of equivalent electrons having binding energy u_i. The result is to be averaged over the speed distributions of the bound electrons, $f_i(v_{2i})$. If we use a hydrogenic speed distribution,

$$f(v_2) = (32/\pi)v_2^2 v_0^5 (v_2^2 + v_0^2)^{-4}, \tag{3}$$

and set

$$n_i = \delta_{1i}, \quad u_i \equiv u_{\text{H}}\,(= \tfrac{1}{2}mv_0^2),$$

we obtain the ionization cross section for hydrogen in this approximation. In Fig. 1, we compare this total ionization cross section, for electron impact, to Born-approximation calculations[8] for various excited states of the bound electron. It should be noted that the speed distribution given by (3) is the exact quantum distribution for a hydrogen atom with any principal quantum number, averaged over all angles.[9] It is also the correct classical distribution, as can be seen by using a microcanonical ensemble.[4] As the principal quantum number increases, the agreement between Born and classical estimates improves, in accord with the results of Ref. 6. At much higher energies, the Born approximation acquires an $(\ln E)/E$ rather than $1/E$ dependence on incident energy, but these differ only slightly at these high energies (see Fig. 2 of Ref. 3).

Since the classical formulation requires strict conservation of energy and momentum between the incident ion and the bound electron, expression (1) is also the differential cross section for acquisition of energy ΔE by the bound electron. That expression can be written as a universal function involving only velocity and energy ratios, thus providing scaling laws. This is also true of the integrated cross sections. Because the expressions for electron impact can be simplified substantially, we discuss electron and heavy-particle impact separately, though it will be seen that the scaling laws are the same for both cases.

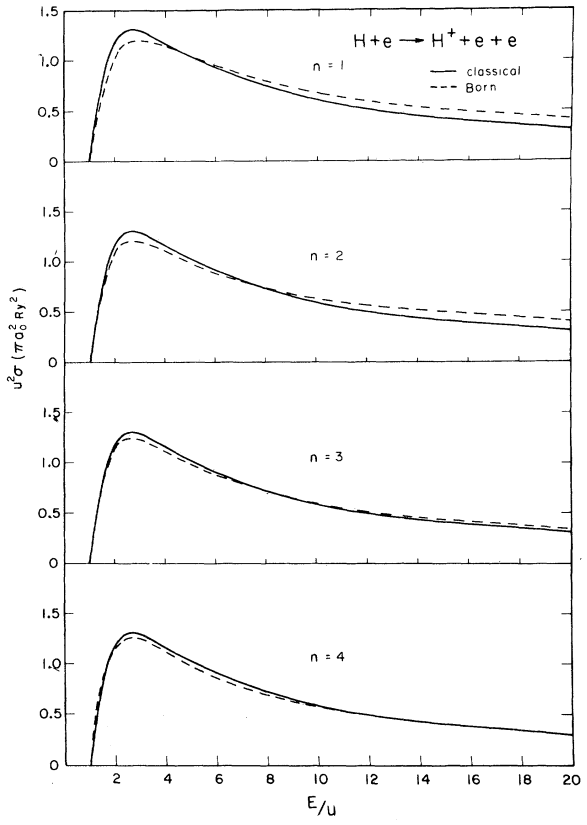

FIG. 1. Total ionization cross sections for ionization of hydrogen atoms in various excited states by electron impact. Solid curves, classical values; dashed curves, Born approximation.

A. Electron Impact

For ionization by electron impact, $m_1 = m_e$, we see that (1) reduces to

$$\frac{d\sigma}{d\Delta E} = \frac{\pi}{3}\frac{e^4}{(\Delta E)^3}\frac{4v_2^2 + 6\frac{\Delta E}{m_e}}{v_1^2}, \quad u < \Delta E < E_1 - E_2;$$

$$= \frac{\pi}{3}\frac{e^4}{(\Delta E)^3}\left(v_1^2 - \frac{2\Delta E}{m_e}\right)^{1/2}\frac{\left(4v_1^2 - \frac{2\Delta E}{m_e}\right)}{v_1^2 v_2}, \quad \Delta E > E_1 - E_2;$$

$$= 0, \quad \Delta E > E_1; \tag{4}$$

where $u = \frac{1}{2} m_e v_0^2$ is the initial binding energy of the ejected electron. To obtain the cross section for ejection of an electron with a final kinetic energy

$$E_2' = \tfrac{1}{2} m_e v^2 = \Delta E - u,$$

we average (4) over the initial bound-state velocity distribution. If a hydrogenic distribution (3) is used, we can write the result in terms of $\beta_1 = E_1/u$, $\epsilon = \Delta E/u = E_2'/u + 1$:

$$d\sigma/dE_2' = \tfrac{2}{3}(e^4/u^3)\epsilon^{-3}\beta_1^{-1} \times\{ (3\epsilon + 4)[\tan^{-1} y + y/(1+y^2)] + [y/(1+y^2)^2](2\epsilon - 8)\}, \quad (5)$$

where $\gamma^2 = \beta_1 - \epsilon$.

It is evident from (5) that $d\sigma/dE_2'$ is a function only of energy ratios, aside from the factor $1/u^3$. Thus, the cross section for ejection of an electron whose binding energy is u_a is related to that for binding energy u_b by

$$\frac{d\sigma(E_1, u_b)}{dE_2'} = \frac{u_a^3}{u_b^3} \frac{d\sigma(E_1^*, u_a)}{dE_2'^*}, \quad (6)$$

where $E_1^* = (u_a/u_b)E_1$, and $E_2'^* = (u_a/u_b)E_2'$.

Speed distributions other than hydrogenic are of some interest. We will deal with only two others here. First, we consider a δ-function speed distribution for the initial bound state corresponding to the virial-theorem (vt) result for the Coulomb force,

$$f_{\mathrm{vt}}(v_2) = \delta(v_2 - (2u/m_e)^{1/2}). \quad (7)$$

This yields, for the ejected electron energy profile, written in the same notation as for (5),

$$\frac{d\sigma_{\mathrm{vt}}}{dE_2'} = \frac{\pi e^4}{3u^3\beta_1\epsilon^3}(4+3\epsilon), \quad 0 < E_2' < E_1 - 2u;$$

$$= \frac{\pi e^4}{3u^3\beta_1\epsilon^3}(\beta_1 - \epsilon)^{1/2}(4\beta_1 - \epsilon), \quad E_1 - u > E_2' > E_1 - 2u;$$

$$= 0, \quad E_2' > E_1 - u; \quad (8)$$

The other distribution, primarily of historical interest, is that implied by the Thomson ionization cross section[10]

$$f_T(v_2) = \delta(v_2), \quad (9)$$

which results in

$$\frac{d\sigma_T}{dE_2'} = \frac{\pi e^4}{u^3\beta_1\epsilon^2}, \quad 0 < E_2' < E_1 - u . \quad (10)$$

We note that both (5) and (8) approach the value given by (10) when $E_1 \to \infty$. These distributions all peak at zero ejected electron energy, as do the quantum results.

In Fig. 2 we compare the correct classical result (5) which the Born calculations of Omidvar,[8] for $E_1 = 9u_{\mathrm{H}}$. Because of the scaling law (6), the classical results predict a universal curve for $u^3 \times d\sigma/dE_2'$ versus E_2'/u, for fixed E_1/u. The corresponding scaling of the total ionization cross section (5) was displayed in Fig. 1; the curves were drawn separately only to display the convergence. It can be seen that even for a principal quantum number as low as $n = 3$, the classical and quantum energy distributions agree quite well. This indicates that the agreement seen in Fig. 1 is not accidental.

The cross section for production of an ejected electron with a final velocity magnitude v is related to $d\sigma/dE_2'$ by

$$d\sigma/dv = (m_e v)\, d\sigma/dE_2' \quad (11)$$

The velocity profiles thus go to zero for zero ejection velocity. The cross sections (11) also scale; this time $u^{5/2}(d\sigma/dv)$ is a universal function of E_2'/u (or v/v_0) and E_1/u. This function, obtained by using (5) in (11), is displayed in Fig. 3

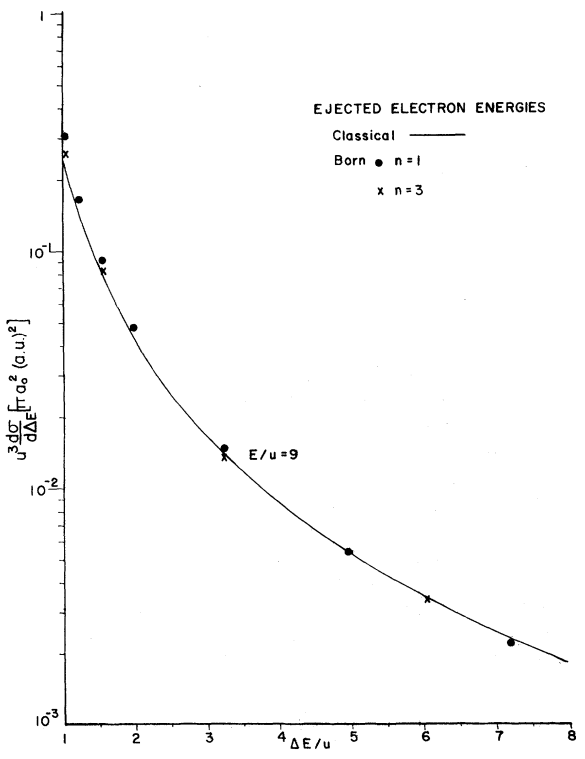

FIG. 2. Ejected electron energy distributions from ionization of hydrogen atoms by electron impact. Solid curve, classical values; circles, Born approximation, ground state; crosses, Born approximation for states with principal quantum number 3.

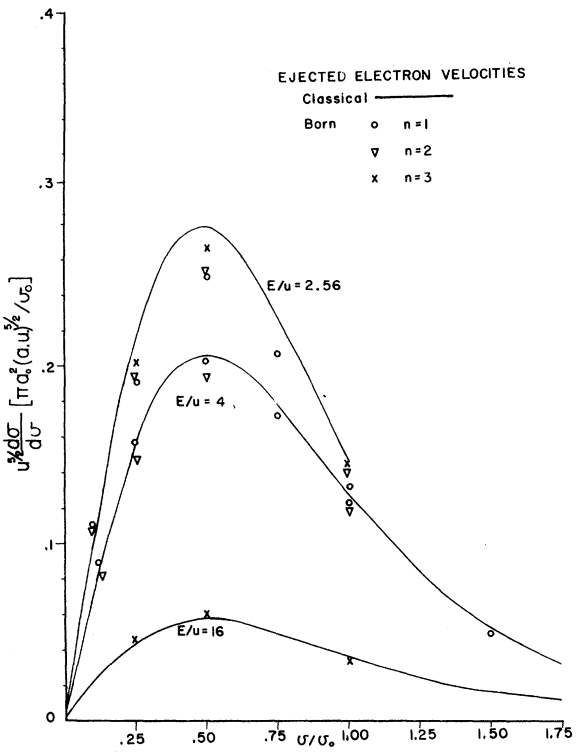

FIG. 3. Ejected electron velocity distributions from ionization of hydrogen atoms by electron impact, for various incident energies. Solid curves, classical values; circles, Born approximation, ground state; triangles, Born approximation, $n=2$; crosses, Born approximation, $n=3$.

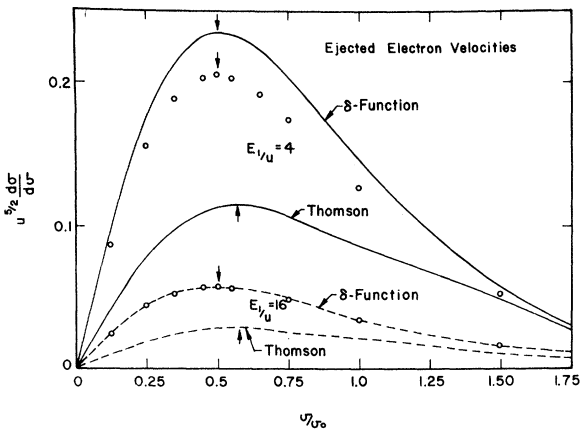

FIG. 4. Effect of initial bound-state velocity distributions on the probability of ejection with a given final velocity. Solid curves, virial theorem and Thomson distributions for incident electron energy of $4u$; dashed curves, $E/u=16$; circles, values using hydrogenic bound-state distributions.

for various values of E_1/u, together with the Born calculations. It is evident that the convergence at low-impact energies is not as good, but for $E \gg u$, the agreement is excellent. Even at low energies, however, the differences amount to less than 15%.

For comparison, we show in Fig. 4 the virial theorem and Thomson profiles. The curves marked δ function are the virial-theorem results (8) used in Eq. (11), and those marked Thomson are those using (10) in (11). The circles are the hydrogenic results (5) used in (11). While it is true that at high energies the results of all three velocity distributions approach each other, we see that this convergence is quite slow. On the other hand, the virial-theorem results are essentially identical with the hydrogenic velocity distribution results by $E_1/u=16$. Again, for large ejection-velocity magnitudes, the curves approach each other. A comparison of Figs. 3 and 4 indicates that the simpler virial-theorem results are adequate representations of the Born approximation for the higher-excited-state ionizations at higher energies.

It is interesting to note that for hydrogen, both the Born approximation and the correct classical approximation predict a peak of the ejected-electron velocity profile at a speed of $v=v_0/2$, where $v_0=(2u/m_e)^{1/2}$, for incident energies larger than $2u$. Since the Born results are numerical evaluations, the interpretation is obscured. From Fig. 4, it is evident that this is a direct result of the bound-electron distribution – in addition, of course, to the Coulomb cross section. (In the present work, that is the only other ingredient.) In fact, we can find the peaks of the distributions directly from differentiating our expressions for (11). While the hydrogenic distribution results are somewhat complicated, the distribution (7) gives, for $E_1>2u$,

$$\frac{d}{dv}\left(\frac{d\sigma_{\mathrm{vt}}}{dv}\right)=0,$$

for $E_2'/u=(\sqrt{232}-13)/9$, $v/v_0\simeq 0.497$,

whereas, assuming with Thomson a zero initial velocity results in

$$\frac{d}{dv}\left(\frac{d\sigma_T}{dv}\right)=0, \quad \text{for } v/v_0=1/\sqrt{3}=0.577.$$

Thus, any bound-electron distribution consistent with the Coulomb force appears to correctly predict the peak position.

Because of the fact that the virial-theorem results approach the Born results at higher energies, we can give a simple expression for the magnitude of $d\sigma/dv$ at its maximum:

$$\left.\frac{d\sigma_{\mathrm{vt}}}{dv}\right|_{\max}=\frac{0.936}{u^{3/2}E_1} \text{ in units of } \frac{\pi a_0^2}{v_0}, \tag{12}$$

where E_1, u are in atomic units (27.2 eV). This should be quite close to the Born result for $E_1/u\gg 1$, and within a factor of 2 for all $E_1/u>2$.

B. Heavy-Particle Impact

For heavy charged particles, the full expression (1) must be used. We present the result of averaging over the virial-theorem distribution (7) in units of πa_0^2/a.u. for an incident charged particle of charge Z, mass $m_1 = m_e/\lambda$, and velocity $v_1 = \alpha v_0$:

$$\frac{d\sigma}{dE_2'} = \frac{Z^2}{3u^3\epsilon^3}\frac{4+3\epsilon}{\alpha^2}, \quad 1<\epsilon<b/u;$$

$$= \frac{Z^2}{6u^3\epsilon^3\alpha^2}[(\alpha+\alpha')^3 - (\gamma-1)^3],$$

$$b/u<\epsilon<a/u;$$

$$= \frac{Z^2\alpha'}{3\epsilon^3\alpha^2}\frac{(4\alpha^2-\lambda\epsilon)}{u^3}, \quad \epsilon>a/u,$$

$$\alpha<2\lambda/(1-\lambda);$$

$$= 0, \quad \epsilon>a/u; \quad \alpha>2\lambda/(1-\lambda) \text{ or } \epsilon>\beta_1; \qquad (13)$$

where $\epsilon = (E_2' + u)/u$, $\alpha' = (\alpha^2 - \lambda\epsilon)^{1/2}$,

$\gamma = (1+\epsilon)^{1/2}$,

$b/u = 4(\alpha+\lambda)(\alpha-1)/(1+\lambda)^2$,

and $a/u = 4(\alpha-\lambda)(\alpha+1)/(1+\lambda)^2$.

In this notation, the energy of the incident particle is $E_1 = \alpha^2 u/\lambda$. It can be seen from (13) that the scaling law (6) applies for heavy particles also, a fact which remains true with hydrogenic distributions as well.

The average over a hydrogenic distribution can also be obtained in closed form directly from (1), as can the averaged total cross sections for ionization of hydrogen by both electron and heavy-particle impact.[11] However, the results are algebraically messy, and programming of Eq. (1) for numerical integration is quite simple. Furthermore, in the heavy-particle case, the energies of interest are in general very much larger than u, so that the use of (13) will differ only slightly from that for a hydrogenic distribution (see Sec. III). The velocity profiles are again obtained by using (11).

These velocity distributions also peak at $v/v_0 = \frac{1}{2}$, provided either (3) or (7) is used for the initial bound-state speed distribution. This merely reaffirms the conclusion that the position of peak of $d\sigma/dv$ reflects only the bound-state speed distribution. No velocity profiles for heavy-particle impact are presented; they are very similar to those shown in Figs. 3 and 4.

It should be noted that the virial-theorem results display a "false cutoff" at large ejected electron energies. This arises from the fact that a heavy charged particle cannot classically transfer a large fraction of its energy to a lighter slower one, as indicated by the zero cross section for the fourth range of values in Eq. (13). The total cross section[1,3] reflects a similar "false cutoff." This is not the case for hydrogenic distributions. As will be seen below, for ejected electron energies smaller than this cutoff, the results given by (13) approximate quite well the hydrogenic distribution results.

III. COMPARISON WITH EXPERIMENT

No experimental results are known to us for ejected electron distributions for electron-impact ionization. Proton-ionization data are available for ionization of H_2 and He.[12,13] Figure 5 depicts the ejected-electron energy profile for 100 keV protons incident on helium atoms. The dashed curve is the classical binary-encounter result (13). Helium has two equivalent electrons, so the results have been multiplied by 2. The crosses indicate the binary-encounter predictions averaged over a hydrogenic velocity distribution (3). As expected, it differs hardly at all from the virial-theorem result until the "false cutoff" energy is reached. The solid curve is a Born calculation for hydrogen, scaled according to (6) and multiplied by n_e (see Ref. 12). It is evident that the binary-encounter approximation represents well the experimental results over five orders of magnitude of cross section change. The comparisons for total cross sections can be found in Ref. 3. Figures 6 and 7 show comparisons using only the virial-theorem distribution (7), for protons on He at 200 and 300 keV, respectively. The solid curves are in both cases scaled Born results for hydrogen. In Fig. 8, we show $d\sigma/dE_2'$ for

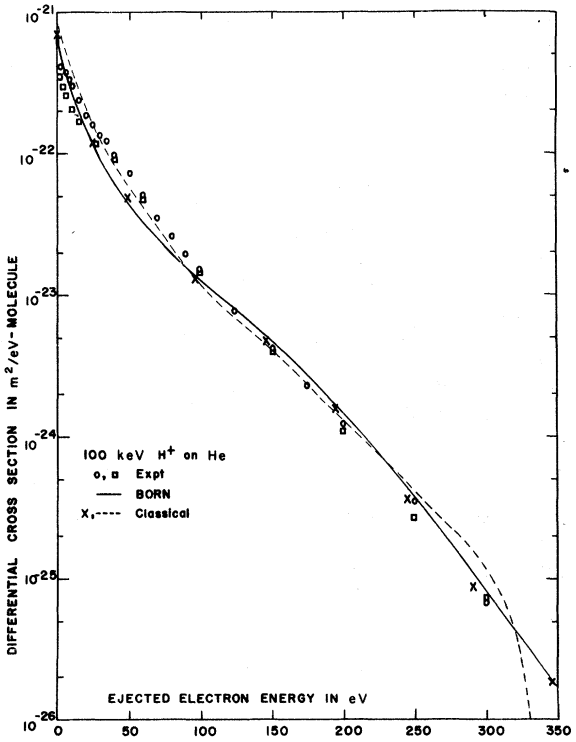

FIG. 5. Ejected electron energy distribution from ionization of He by 100 keV protons. Circles and squares, experiment (Refs. 12 and 13); crosses, classical using hydrogenic bound-state distributions; dashed curve, classical using virial-theorem distribution; solid curve, scaled Born approximation.

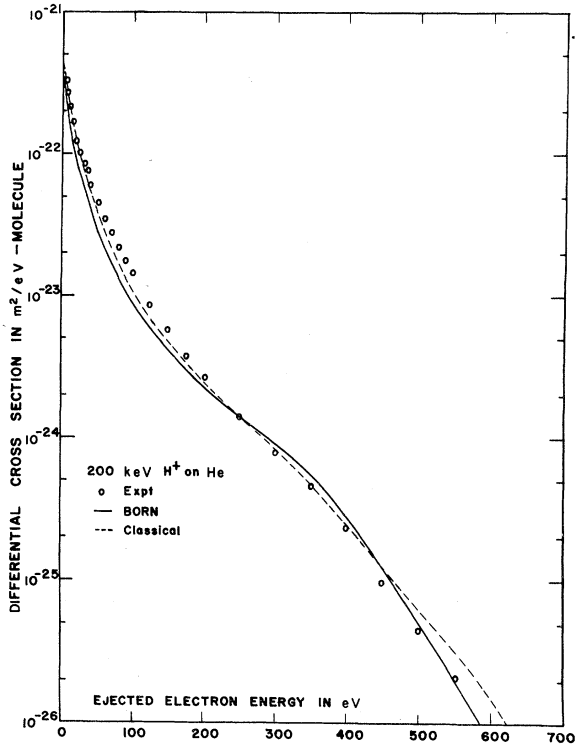

FIG. 6. Ejected electron energy distribution from ionization of He by 200 keV protons. Circles, experiment (Ref. 12); solid curve, scaled Born approximation (Ref. 12); dashed curve, classical.

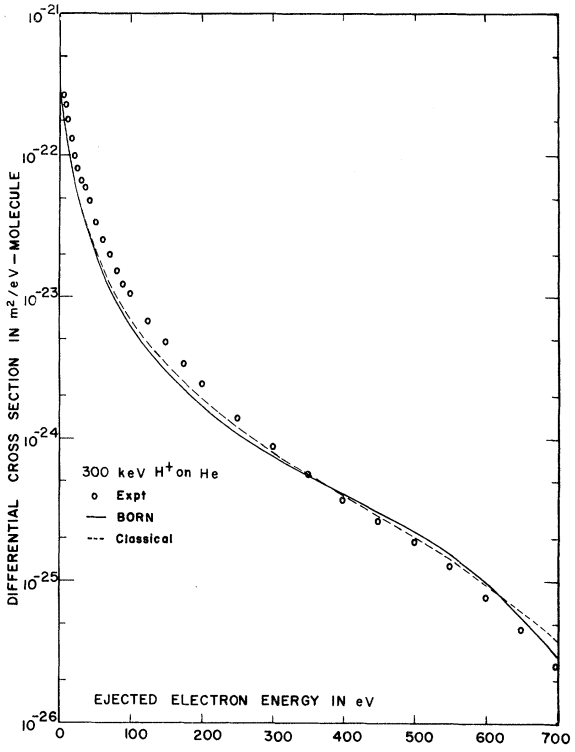

FIG. 7. Same as Fig. 6, for 300 keV protons.

100 keV protons incident on hydrogen molecules. The solid curve is again a scaled Born approximation, while the broken curve is the virial-theorem result. For comparison, we have included (dashed curve) the results predicted using Gryzinski's approximate expression,[1] for a bound-electron distribution as in (7). It can be seen that the approximations he introduces, even excluding his use of an exponential bound-state distribution, distort the classical results somewhat. In fact, the classical results are in good agreement with at least a scaled Born approximation. Though our comparisons extend only so far as the data, it would be interesting to see how well the hydrogenic results hold up at higher ejected electron energies. At much higher energies, the classical will be slightly larger than the Born values.

IV. DISCUSSION

Some remarks are in order concerning the application of this model to larger systems. Because of the scaling laws, these results are readily generalized to any atomic system, by simply adding up the contributions from each atomic shell. It should be recognized, however, that the results so obtained will be only the direct contributions to the resultant ejected-electron distributions. In the alkalis, for example, the inner-shell contributions dominate the cross sections.[2] This implies subsequent Auger transitions, which will produce ejected-electron spectra of a completely different character.

The smooth characteristics of $d\sigma/dE_2'$ suggest that it may be possible to use the present predictions to remove the direct process background to obtain better estimates of the multiply excited-state positions and strengths.[14] The velocity profiles, on the other hand, will have peaks corresponding to the various inner-shell direct ejections. Since the energies of these shells are not always well known, and since coincidences of peaks may occur, the interpretation would be made difficult.

The evidence accumulated to date leads to the conclusion that the direct ionization of atoms and simple molecules can be quite satisfactorily explained as a binary encounter process. Furthermore, since the final state is already one in which classical analysis is valid, the correspondence principle becomes operative for initial states much lower than might otherwise be expected. In fact, it appears as if the ground state of hydrogen is anomalous in this respect. However, it is also clear that quantum effects remain quite important for incident energies near threshold. For such energies, the exchange effect, among others, is not small; neither a simple Born nor a classical approximation can be valid, though it does appear that they are not in error even there by factors larger than about 2. In every ionization reaction examined thus far, the classical binary-encounter

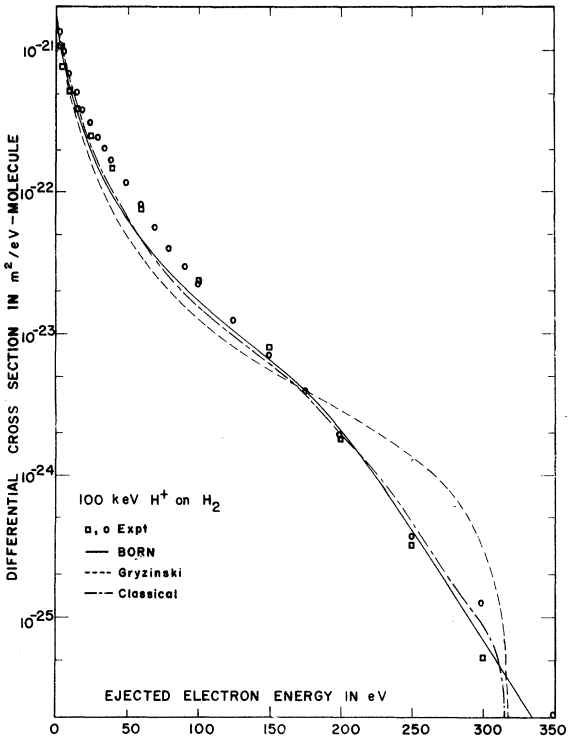

FIG. 8. Ejected electron energy distributions from ionization of hydrogen molecules by 100 keV protons. Circles and squares, experiment (Refs. 12 and 13); solid curve, scaled Born approximation (Ref. 12); broken curve, classical; dashed curve, Gryzinski approximation to classical values.

analysis appears as reliable as a first Born estimate, and has the advantage of being analytically much simpler.

ACKNOWLEDGMENT

The University of Arizona Computer Center made CDC 6400 time available for certain of the results reported herein.

*Supported in part by National Aeronautics and Space Administration and by U. S. Office of Naval Research.

[1]M. Gryzinski, Phys. Rev. 138, A336 (1965).

[2]E. Bauer and C. D. Bartky, J. Chem. Phys. 43, 2466 (1965); J. D. Garcia, J. Chem. Phys. 47, 3679 (1967).

[3]J. D. Garcia, E. Gerjuoy, and J. E. Welker, Phys. Rev. 165, 66 (1968).

[4]R. Abrines and J. C. Percival, Proc. Phys. Soc. (London) 88, 873 (1966); 89, 515 (1966).

[5]A. E. Kingston, Phys. Rev. 135, A1537 (1964).

[6]J. D. Garcia, Phys. Rev. 159, 39 (1967).

[7]E. Gerjuoy, Phys. Rev. 148, 54 (1966). In Ref. 1, Gryzinski also derives this cross section, but uses both simplifying and dynamical assumptions, some of which are unjustified. L. Vriens, Proc. Phys. Soc. (London) 90, 935 (1967), also derives this cross section, but with the approximation $m_e/m_1 \rightarrow 0$. Expression (1) is classically correct.

[8]K. Omidvar, Phys. Rev. 140, A26 (1965). Omidvar also compares his result to a classical estimate; however, he uses the results of Gryzinski (Ref. 1), which contain an unjustifiable exponential velocity distribution. It can be seen from Fig. 1 that the correct classical results compare much more favorably with the quantum results as n increases.

[9]V. Fock, Z. Physik 98, 145 (1935).

[10]See, for example, R. C. Stabler, Phys. Rev. 133, A1286 (1964). Stabler shows the relation of the Thomson cross section to (4), and also a comparison of the resultant total cross sections.

[11]B. K. Thomas and J. D. Garcia, unpublished.

[12]M. E. Rudd, C. A. Sautter, and C. L. Bailey, Phys. Rev. 151, 20 (1966).

[13]M. E. Rudd and T. Jorgensen, Jr., Phys. Rev. 131, 666 (1963).

[14]Our calculations for proton-impact ionization of Ar, for example, indicate the character of $d\sigma/dE_2'$ is much the same as that displayed here.